RESEARCH FRONT

CSIRO PUBLISHING

Journal of Southern Hemisphere Earth Systems Science, 2020, **70**, 120–138
https://doi.org/10.1071/ES20001

Seamless climate change projections and seasonal predictions for bushfires in Australia

Andrew J. Dowdy

Bureau of Meteorology, Victoria, Australia. Email: andrew.dowdy@bom.gov.au

Abstract. Spatio-temporal variations in fire weather conditions are presented based on various data sets, with consistent approaches applied to help enable seamless services over different time scales. Recent research on this is shown here, covering climate change projections for future years throughout this century, predictions at multi-week to seasonal lead times and historical climate records based on observations. Climate projections are presented based on extreme metrics with results shown for individual seasons. A seasonal prediction system for fire weather conditions is demonstrated here as a new capability development for Australia. To produce a more seamless set of predictions, the data sets are calibrated based on quantile-quantile matching for consistency with observations-based data sets, including to help provide details around extreme values for the model predictions (demonstrating the quantile matching for extremes method). Factors influencing the predictability of conditions are discussed, including pre-existing fuel moisture, large-scale modes of variability, sudden stratospheric warmings and climate trends. The extreme 2019–2020 summer fire season is discussed, with examples provided on how this suite of calibrated fire weather data sets was used, including long-range predictions several months ahead provided to fire agencies. These fire weather data sets are now available in a consistent form covering historical records back to 1950, long-range predictions out to several months ahead and future climate change projections throughout this century. A seamless service across different time scales is intended to enhance long-range planning capabilities and climate adaptation efforts, leading to enhanced resilience and disaster risk reduction in relation to natural hazards.

Keywords: bushfires, climate change projections, climate extremes, dangerous weather conditions, disaster risk reduction, natural hazards, seasonal predictions, wildfires.

Received 19 July 2020, accepted 7 December 2020, published online 17 December 2020

1 Introduction

Fire weather prediction data are needed for a range of purposes in Australia, including for short-range bushfire management decisions, as well as long-term planning. Data and derived guidance products that have consistency over different time scales can have practical benefits for decision-makers, such as for integrated system planning (e.g. as used in the energy sector in Australia) covering a range of time periods into the future, given that values from different data sets can be more directly used in combination with each other. Consequently, this type of seamless information for predictions over different time scales can help enable effective preparedness for natural hazards such as bushfires.

This paper describes recent research on seamless predictions over different time scales, including covering climate change projections for bushfire weather indices as well as seasonal predictions of fire weather conditions, all made to be consistent with a historical data set of daily gridded values back to 1950. Development of seamless fire weather guidance products for Australia has been underway for several years now (Dowdy *et al.* 2017; Dowdy 2019). This current study is based on results presented in a research and development workshop held at the Bureau of Meteorology (BoM) in November 2019 titled 'Forecasting for the future: New science for improved weather, water, ocean and climate services' as detailed in Bureau of Meteorology (2019), with this paper forming part of a special edition of this journal intended for publishing the research presented at that workshop. The results presented here are part of long-term efforts that have been underway to produce seamless information for various natural hazards over all time scales including from historical data based on observations, long-range multi-week to seasonal predictions, as well as future projections of climate change in coming years and decades. A range of fire weather products covering these time scales are described here.

Climate change projections for fire weather conditions in a warmer world have been produced based on global climate model (GCM) data and calibration methods as presented in several previous studies for Australia (CSIRO and BoM 2015; Dowdy *et al.* 2019). Dynamical downscaling approaches have also been used to produce finer-scale information from the GCM data, including for examining projections of future fire weather conditions (Clarke *et al.* 2016; Di Virgilio *et al.* 2019).

Methods have been developed for various regions of the world for seasonal prediction of wildfire risk factors (Chen *et al.*

2016; Garfin *et al.* 2016; Chikamoto *et al.* 2017; Bedia *et al.* 2018; Turco *et al.* 2018). Research has demonstrated that Australia is a lucky country in relation to having a relatively high level of predictive skill for fire weather conditions several months in advance in some regions/seasons when compared to most other regions of the world for which the predictive skill is generally not as high (e.g. >80% accuracy for predicting above or below median seasonal values in eastern Australia during spring; Dowdy *et al.* 2016). Some of this skill for predicting risk factors for bushfires in Australia relates to the influence of large-scale atmospheric and oceanic modes of variability such as the El Niño-Southern Oscillation (ENSO), Indian Ocean Dipole (IOD) and Southern Annular Mode (SAM) which help provide predictability for weather factors, including over spring and the warmer months of the year in Australia when dangerous fires more frequently occur (Williams *et al.* 2001; Nicholls and Lucas 2007; Dowdy *et al.* 2016; Harris and Lucas 2019; Harris *et al.* 2019). Additionally, recent research has demonstrated that sudden stratospheric warming events over Antarctica during winter and early spring provide a source of predictability for fire weather conditions in Australia in subsequent months (Lim *et al.* 2019).

Although studies such as these have demonstrated that fire weather conditions are predictable in Australia at multi-week to seasonal lead times, long-range predictions of fire weather indices have not previously been developed for providing guidance to fire agencies in Australia, as existing capabilities developed in BoM have been around providing individual temperature and rainfall products for those time scales as guidance for fire agencies. A new system for providing long-range fire weather guidance up to several months ahead is demonstrated here, based on fire weather indices that combine wind speed, humidity, temperature, rainfall and pre-existing fuel moisture information.

This study presents results based on model data over a range of different time scales, including based on GCM data for future climate change projections as well as from the ACCESS-S1 model currently used in BoM for seasonal prediction capabilities (Hudson *et al.* 2017). In particular, the McArthur Forest Fire Danger Index (FFDI) is used here for indicating weather conditions associated with the potential for hazardous bushfire events (McArthur 1967). The GCM data and ACCESS-S1 data are all calibrated to be consistent with the same historical FFDI data set. Details on data and methods are provided in Section 2, with results presented in Section 3 and conclusions in Section 4.

2 Data and methods

2.1 Data sets

Eqn 1 shows the calculation for the McArthur Mark V FFDI (McArthur 1967; Noble *et al.* 1980) using daily maximum temperature at a height of 2 m (T), mid-afternoon values of relative humidity at a height of 2 m (RH), mid-afternoon values of wind speed at a height of 10 m (W) as well as a drought factor (DF) representing fuel availability based on a soil moisture deficit. The Keetch Byran Drought Index (KBDI; Keetch and Byram 1968) is used here for the soil moisture deficit, calculated from daily rainfall and daily maximum temperature at a height of 2 m. For the climate model data (including ACCESS-S1 and GCM data), relative humidity and wind speed values at 0600 UTC are used to represent mid-afternoon values for Australia. A data set of FFDI values primarily based on a gridded analysis of observations is also used here, with a grid of 0.05° in latitude and longitude throughout Australia, as detailed in Dowdy (2018). The FFDI is used here as a broad-scale general indicator of fire weather conditions, with results interpreted based on the FFDI being a useful way of combining these weather factors that can influence bushfire danger in Australia.

$$\mathrm{FFDI} = 2e^{(0.0338\,\mathrm{T}+0.0234\,\mathrm{W}-0.0345\,\mathrm{RH}+0.987\ln(\mathrm{DF})-0.45)} \quad (1)$$

GCM data are available in conjunction with the Intergovernmental Panel on Climate Change (IPCC), based on a set of GCM experiments: the Coupled Model Intercomparison Project phase 5 (CMIP5) (Taylor *et al.* 2012). The output from 15 of those GCMs was recently used to produce projections of the FFDI for each day out to 2100 throughout Australia, as detailed in Dowdy *et al.* (2019). Quantile matching was used to calibrate those GCM-based FFDI data so that they were consistent with the historical observations-based FFDI data set (Dowdy 2018), as described in Section 2.2. The 15 GCMs are ACCESS1-0, ACCESS1–3, BCC-CSM1-1, BCC-CSM1-1-M, BNU-ESM, CCSM4, CNRM-CM5, CSIRO-Mk3–6-0, FGOALS-G2, GFDL-CM3, GFDL-ESM2G, GFDL-ESM2M, MIROC5, MRI-CGCM3 and NorESM1-M. For further details on these models see Appendix Table A1 and Moise *et al.* (2015). A high emission pathway was used for those projections (RCP8.5, with no stabilisation this century leading to about 1370 ppm CO_2 equivalent by 2100) so as to examine the influence of increased greenhouse gas concentrations.

Long-range model predictions (at multi-week to seasonal lead times) are produced in Australia for weather conditions such as temperature and rainfall based on output from ACCESS-S1, the BoM's seasonal forecasting model (Hudson *et al.* 2017). This includes an ensemble of hindcast model runs from 1990–2012, as well as an ensemble of real-time model runs also available for predictions out to several months ahead. Post-processed data are available for various weather variables such as temperature, rainfall and atmospheric moisture content (vapour pressure) calibrated using quantile matching for consistency with observations-based gridded data sets such as those described in Jones *et al.* (2009), including for the input variables of the FFDI (from Eqn 1) consistent with the historical gridded FFDI data set described by Dowdy (2018). Quantile matching based on ACCESS-S1 uses the hindcast data for the training period, based on the combined probability density function of all 11 members for the years 1990–2012 that comprise the hindcast data.

Previous examinations used calibrated ACCESS-S1 hindcast data for FFDI and demonstrated a useful level of predictive skill (including for indicating the likelihood of FFDI values being above the historical mean values) (Dowdy *et al.* 2017; Dowdy 2019). Building on those previous results using calibrated hindcast data from ACCESS-S1, this study presents long-range FFDI predictions based on the calibrated real-time data from ACCESS-S1.

The results presented in this study are for the real-time ACCESS-S1 model run that was initialised at the start of

November 2019, using ensemble members from 1 to 50 (i.e. a 50-member ensemble), with the full set of 100 members intended to be used in the future for this system. Calibrated values of daily maximum temperature, daily rainfall, daily wind speed and vapour pressure for 1500 UTC are used, with the vapour pressure data used together with daily maximum temperature for indicating mid-afternoon relative humidity values and wind speed calibrated to match that of the historical gridded FFDI data set (Dowdy 2018) using the quantile matching approach described in Section 2.2. Predictions of FFDI were calculated for each day out to the end of February 2020 for each individual ensemble member. Details on the suite design are provided in Section 3.2, as well as examples of the fire output products produced using this objective long-range prediction system for Australia. This includes guidance products provided to fire agencies around Australia prior to the 2019–2020 summer fire season, noting the devasting effects of the extreme fire weather conditions that eventuated (Bureau of Meteorology 2020) and the disastrous impacts that the fires ended up having on Australian society and environment (Boer *et al.* 2020; Johnston *et al.* 2020; Ward *et al.* 2020).

Seasonal averages of data through the study are used for December, January and February (DJF), March, April and May (MAM), June, July and August (JJA) and September, October and November (SON). Large-scale modes of variability are considered, including the ENSO (as represented by the NINO3.4 index) and the IOD (as represented by the Dipole Mode Index, DMI). Data for these indices are based on sea-surface temperature (SST) data obtained from the National Oceanic and Atmospheric Administration (NOAA) (http://www.cpc.ncep.noaa.gov/, accessed August 2017).

2.2 Quantile matching method

Details on the quantile matching method were provided in Dowdy (2019), including the steps that comprise the method. Those steps are also presented here for reference, as shown below. The method was previously applied to GCM data to produce future projections of FFDI values as presented in Dowdy *et al.* (2019), noting that this method was designed for attention to detail around extremes. The steps that comprise this quantile matching for extremes (QME) method are based on matching model data to observations (or reanalysis data) using individual quantile values (i.e. quantile matching is a ranking-based approach). This QME approach was applied for each of the four input variables of the FFDI: daily maximum temperature, daily rainfall, afternoon relative humidity and afternoon wind speed.

Prior to training the QME method, the data from each individual model are bilinearly interpolated for regridding to match that of the observations data. The QME is then applied to the input variables of the FFDI, but not to the resultant FFDI values as they are found to already provide a good match to observations-based data including for high percentile values of FFDI (as detailed in Section 3.1 with results presented for the 95th and 99th percentile values). This was similarly shown in Dowdy *et al.* (2019), their Fig. 4, which also shows comparisons with results based on dynamical downscaling from regional climate model experiments. While acknowledging that a loss of internal physical consistency can be one of the limitations of statistical methods for bias correction, examples such as these help indicate that the QME method is suitable for the purposes of this study, with no sign of substantial issues relating to a loss of internal physical consistency (noting that the higher values of FFDI require simultaneously high values of various input variables to the FFDI).

The following steps are used for training the QME method:

(a) Create probability density functions (PDFs) of weather variable data for a historical training period, including a PDF for the model data and also a PDF for the observations data. This is done individually for each location of interest (e.g. grid cell region). This was done for daily values through the period 1975–2017 for each individual GCM.
(b) Using the rankings of values in these PDFs, a given value of a weather variable for the model data is matched to the corresponding value for the observations-based data, with the matched values having equal rankings in their respective distributions.
(c) The five most extreme values are used to calculate the mean difference between the model and the observations-based data, with this mean difference used for the bias correction applied to values outside of the historical range of occurrence. This is calculated individually for the five extreme high values, as well as for the five extreme low values. This approach allows extreme values of this order to be represented in the model data after this calibration has been applied, while also helping avoid a potentially strong influence in some rare cases from outliers (e.g. if a 1 in 500 year event occurred during the historical training period).

The above steps were applied individually for different seasons (DJF, MAM, JJA and SON), noting that benefits can be obtained from seasonal application of statistical bias correction methods (e.g. Hertig *et al.* 2019). Although quantile matching approaches are typically thought to retain the magnitude ordering of data, applying this method for each individual season allows the magnitude ordering of the data over all seasons to be changed, which can be beneficial for extreme events. For example, different weather systems can preferentially occur around a particular time of year and models can vary in their ability to represent some types of weather phenomena, such that the seasonal application of this method may help account for different biases specific to different weather phenomena to some degree. Additionally, it was found when applying this quantile matching method to temperature projections towards the end of this century (using a high emissions scenario) that the large-scale shift in the overall PDF is important to consider. Consequently, a 40-year running mean anomaly (as compared to the mean value for the historical training period used in Step 1) is subtracted from the future projections of temperature prior to applying the quantile matching method described in the above steps. After the quantile matching has been applied, the 40-year mean anomaly is added back into the data. These steps as described above result in an improved representation of the model data as compared to the observations-based data. Some results of applying the QME method to GCM data were presented in

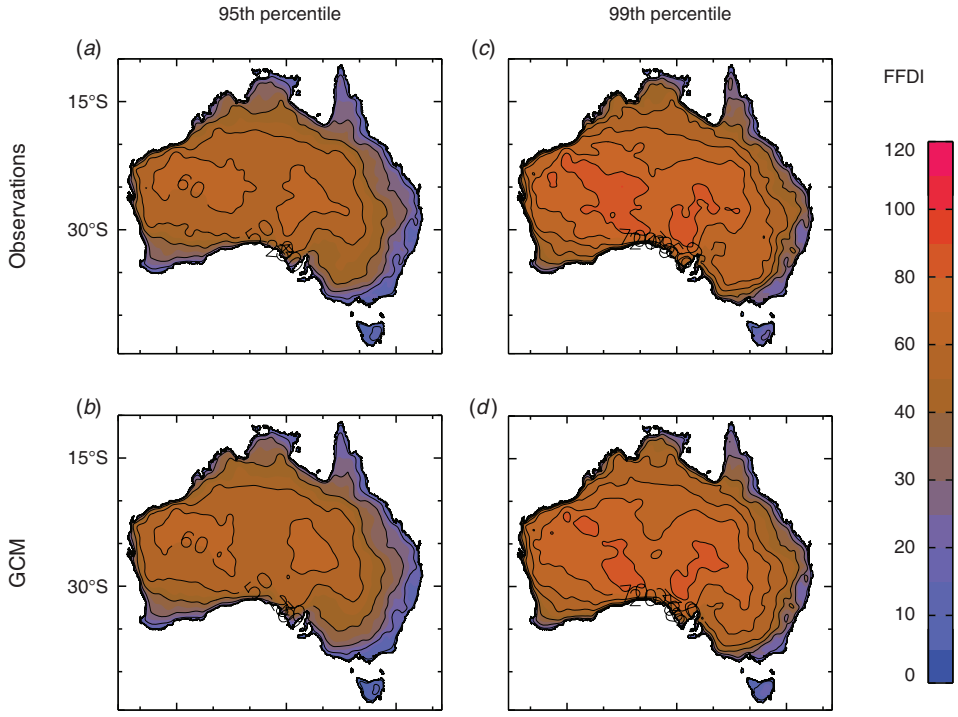

Fig. 1. Historical near-surface fire weather conditions based on daily values of FFDI for the period 1990–2009. The 95th percentile (*a*, *b*) and 99th percentile (*c*, *d*) of the daily FFDI values are shown for the observations-based data (*a*, *c*) as well as for the calibrated GCM data (*b*, *d*).

Dowdy (2019) and Dowdy *et al.* (2019). Some examples of results are also included here in the Appendix Figs A3 and A4.

As noted by Casanueva *et al.* (2020), high-quality observational data sets are essential for comprehensive analyses in larger (continental) domains when trying to account for model biases. A gridded analysis of observations is used in this study obtained from the Australian Water Availability Project (AWAP) data product described by Jones *et al.* (2009), providing data on a grid of 0.05° in latitude and longitude throughout Australia. Assessment of this gridded data set has concluded that it is suitable for broad-scale climate analysis purposes, such as detailed in King *et al.* (2013) who reported that the AWAP product is suitable for use in studies on trends and variability in rainfall (including extremes) across much of Australia, while also noting that a limitation of gridded analyses of observations-based data is the level of spatial detail available in regions where there is a low density of station observations. This is particularly the case in western inland regions of Australia, such that results should be interpreted accordingly (e.g. only broad-scale features are considered when describing and interpreting results for those regions in this study).

3 Results

3.1 Climate change projections

The ensemble of model data from the 15 GCMs with calibration applied (using the QME method described in Section 2.2) produces FFDI values during a historical period that are very similar to those of the historical observations-based data. This is shown in Fig. 1 based on data for the period 1990–2009. The similarities include spatial features of the FFDI magnitude for mean values of the FFDI, as well as for extreme values (e.g. corresponding to the 95th percentile). This is as expected based on the application of this calibration approach, intended to help provide climate change projections information and data that are consistent with the historical FFDI data set.

Projected future changes in the number of days with FFDI exceeding a threshold are shown in Fig. 2, for the period 2060–2079 as compared to the period 1990–2009 under a high emissions pathway (RCP8.5 as described in Section 2.1). Projected changes are presented for the number of days per year with FFDI $>$ 50 corresponding to days classed as Severe (or above) for operational fire weather forecasting purposes, as well as for the number of days exceeding the historical 99th percentile of FFDI, presented for individual seasons of the year.

The projected changes for FFDI $>$ 50 are generally larger in the more inland regions. However, that is generally related to those inland regions having a relatively high number of days with FFDI $>$ 50 during the historical climate when compared to the more coastal regions. In contrast, the projected future change in the number of days exceeding the historical 99th percentile of FFDI is generally more spatially consistent, with an increase of about 2–5 days indicated for many regions of Australia. The largest increases tend to occur during spring (SON) in many northern and northeastern regions and during summer (DJF) in many central and southern regions, noting some similarities to observed trends in recent decades that show larger changes during spring than autumn (Dowdy 2018; Harris and Lucas 2019).

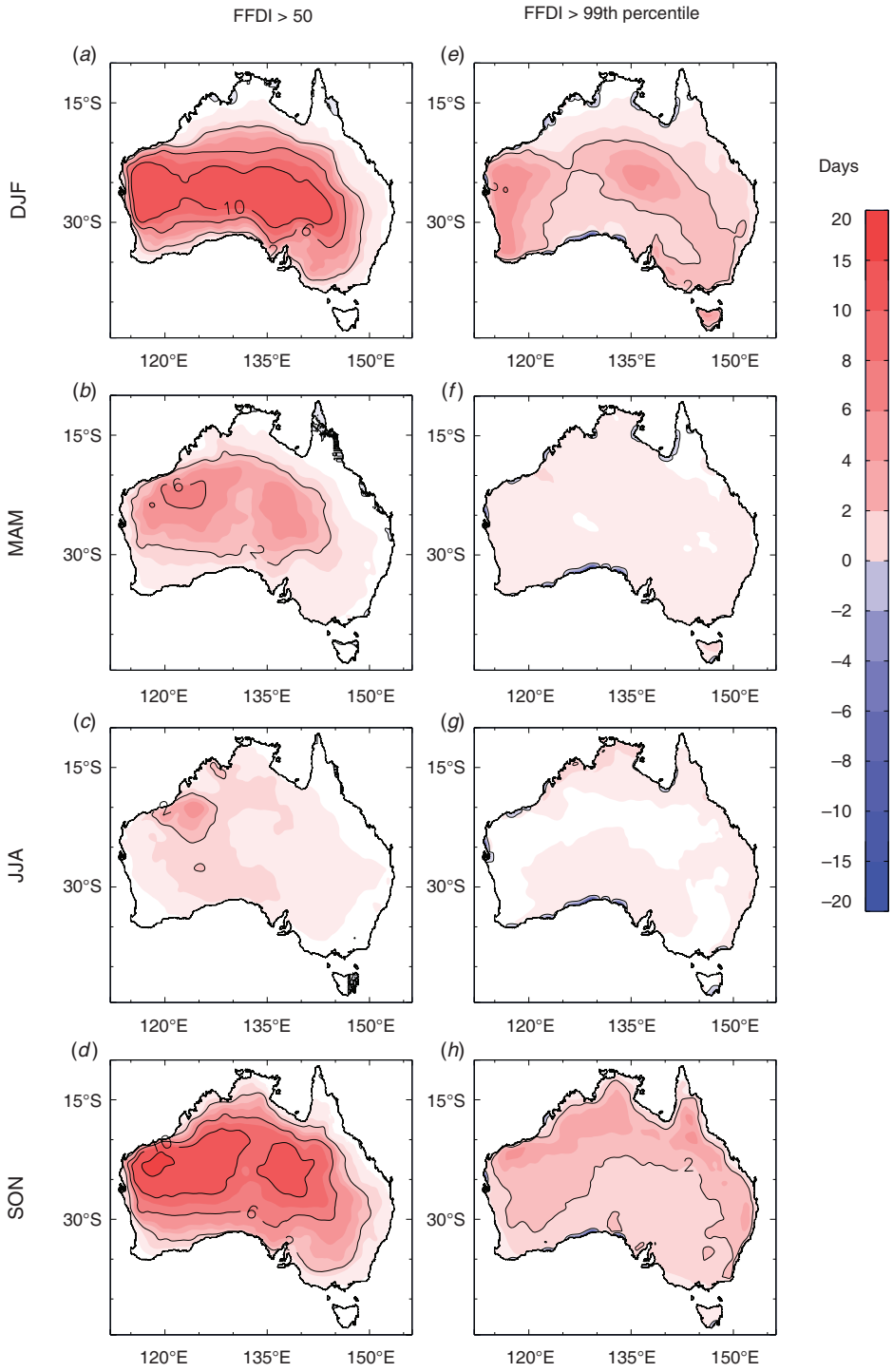

Fig. 2. Future projections in FFDI values from the calibrated GCM data. Changes are shown for the number of days per year that the FFDI exceeds a threshold value, based on changes from the period 1990–2009 to the period 2060–2079. Results are presented for the number of days per year that FFDI is above 50 (left panels, *a*–*d*) and the number of days per year that FFDI is above its historical period 99th percentile (right panels, *e*–*h*). This is shown for individual seasons DJF (*a*, *e*), MAM (*b*, *f*), JJA (*c*, *g*) and SON (*d*, *h*). White regions are where less than two thirds of the ensemble have a consistent direction of projected change.

These projections are examples of the type of information that can now be produced for fire weather measures using calibrated data from these GCMs, based on daily data from 1970 to 2100 on the same 0.05° grids as used for the historical FFDI data set as well as for the ACCESS-S1 FFDI data set. Consequently, there is considerable potential for examining a range of guidance measures, including for changes in mean values or more extreme values (such as using fixed thresholds or percentile/return period type of thresholds as presented in the examples shown in Fig. 2) based on these large multi-member calibrated data sets.

The time periods for the projections presented in this study are somewhat arbitrary, noting that any other time periods from 1970–2099 are also available based on these data. As an example of this, a version of Fig. 2 but for 2020–2039 projections is shown in Appendix A (Fig. A1), generally indicating similar spatial features to Fig. 2 but lower magnitude changes. The various input components to the FFDI also provide scope for improved understanding of projected future changes in various aspects of weather and climate based on calibrated data consistent with observations-based data sets. For example, projected changes in return period values of extreme rainfall can readily be produced based on this long period of available data (i.e. 130 years), such as similar figures to Fig. 2 but for the changes in the frequency of days exceeding the historical 10-year return period or in the frequency of days exceeding FFDI of 100 (classed as 'Catastrophic' or 'Code Red' in some states). Compound hazards could also potentially be examined based on combined wind, humidity and temperature extremes. Projected changes could be examined in vegetation–weather relationships relevant for fire management or agricultural applications, such as things like Goyder's Line as indicated by 220 mm growing season April–October rainfall (Tozer *et al.* 2014) or other measures (Meinig 1961; Nidumolu *et al.* 2012), as well as other biogeographic mapping applications and quantities relevant for other sectors.

Projected changes can also be considered per degree of global warming and scaled accordingly, noting a recent focus on projected changes for 1.5°C and 2°C global warming (IPCC 2018). Lists of global warming values are available for different time periods and emissions pathways, such as table SPM.2 of IPCC (2013) from the IPCC Fifth Assessment Report. Based on global warming values such as those, the projections shown in Fig. 2 (for RCP8.5 from the period 1990–2009 to 2060–2079 for RCP8.5) correspond to about 2.5°C global warming, such that dividing those projections by 2.5 could provide an estimate of the change per degree of warming). The FFDI projections (and seasonal outlooks) presented in this study could be used together with relationships between historical FFDI data (Dowdy 2018) and bushfire impacts (Bradstock *et al.* 2009; Blanchi *et al.* 2010, 2014) to help understand future changes in bushfires and their impacts. Ignition and fuel conditions could also be considered, noting considerable uncertainties around various combinations of factors that cause extremely dangerous fires (i.e. as a form of compound event).

3.2 A system for multi-week to seasonal predictions of fire weather

The predictability of fire weather conditions at multi-week to seasonal time scales is dependent on various factors, including the regular seasonal progression of fire weather conditions over Australia (e.g. Luke and McArthur 1978), pre-existing fuel conditions and large-scale modes of atmospheric and oceanic variability (Nicholls and Lucas 2007; Dowdy 2018; Harris and Lucas 2019) as well as sudden stratospheric warming events over Antarctica (which can influence cloud cover, temperature and rainfall over eastern Australia, thereby influencing fire weather conditions; Lim *et al.* 2019). For the progression of the peak conditions for dangerous fire weather through the year, Fig. 3 shows that for different seasons based on the historical data set from 1950–2016 (Dowdy 2018). This indicates similar features in general to earlier results such as those of Luke and McArthur (1978), acknowledging that they didn't have access to long time periods of daily gridded data based on observations throughout Australia as is now available as well as noting relatively sparse observations network in some parts of Australia (e.g. around the Nullarbor Plain and desert regions to the north of that area through central-west regions of Australia; Jones *et al.* 2009).

In relation to large-scale modes of variability (e.g. ENSO, IOD and SAM), Fig. 4 presents correlation values (Pearson's r) for the individual input ingredients of the FFDI with the NINO3.4 index (representing ENSO conditions), with strong relationships indicated in many regions of Australia particularly during spring (SON) and summer (DJF). It is apparent from Fig. 4 that temperature, humidity and rainfall tend to act in concert with each other (i.e. all corresponding to more dangerous conditions for bushfires when NINO3.4 is high, noting that high positive values of NINO3.4 are characteristic of El Niño events and large negative values characteristic of La Niña events). Wind speed has considerably different spatial features for its ENSO relationship when compared to the other individual weather variables and FFDI in general. It is also noted that the relationship between ENSO and FFDI is clearer in some ways than for its individual input ingredients' relationship with ENSO, which could be expected to some degree given the integrated effect of temperature, humidity and rainfall in the FFDI formulation (Eqn 1). For example, the region of significant correlation during spring covers the majority of the country, for a larger area than is the case for any single weather variable, which appears to be similar to the relationships for rainfall and humidity in northern regions and for temperature in central and southern regions.

The pre-existing fuel moisture is another weather-related factor that can provide some long-range (i.e. >1 week) skill at predicting fire weather conditions. This is because of the rate at which fuel moisture can change (noting slower rates for larger fuel than finer fuel) provides a form of memory with persistence based on past conditions that can influence future conditions. As examined later in this section (as well as in Section 3.3), the 2019–2020 summer had several of these factors occurring in combination with each other that all can exacerbate the severity of fire weather conditions, including leading into the event in spring with a strong IOD event and a stratospheric warming event (that was one of the strongest ever observed in the southern hemisphere) as well as very dry fuel conditions associated with a multi-year drought (Bureau of Meteorology 2020). Consequently, it could be expected that the ACCESS-S1 FFDI values

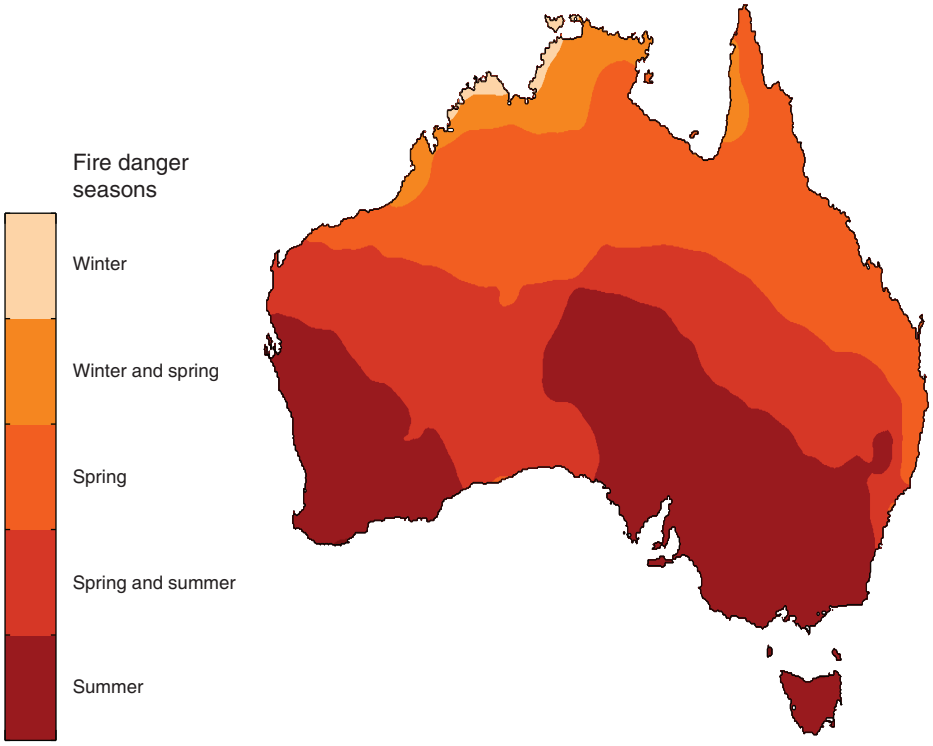

Fig. 3. The season with the most dangerous weather conditions for bushfires, mapped for different regions of Australia. At each location, the season shown is the one with the highest average value of the Forest Fire Danger Index (FFDI, based on daily data from 1950 to 2016 (Dowdy 2018)) with a 100 km smoothing applied to highlight broad-scale regional features. This is shown for winter (averaged for June, July and August), winter and spring (averaged for half of July, August, September and half of October), spring (averaged for September, October and November), spring and summer (averaged for half of October, November, December and half of January) as well as summer (averaged for December, January and February), without notable regions occurring for other season types through the year (summer and autumn; autumn; autumn and winter).

would be indicating more dangerous conditions for bushfires for the period going into summer in many parts of eastern and southern Australia, given that antecedent fuel moisture measures are used based on observations (i.e. KBDI as described above) and that the ACCESS-S1 model can simulate aspects of these large-scale circulation features (Hudson *et al.* 2017).

The Australian Seasonal Bushfire Outlook is routinely released through the Bushfire and Natural Hazards CRC (BNHCRC), with input on some regional risk factors such as fuel conditions provided by fire agencies around Australia, and input from long-range weather and climate predictions provided by BoM. Prior to the development of objective fire weather outlooks for Australia as described in this section, the outlooks were based on considering long-range predictions of temperature and rainfall individually. This new development is a considerable step up from that previous capability, with the new method combining long-range predictions of humidity, wind, temperature and rainfall, together with observations-based estimates used to indicate fuel moisture content.

The design of the objective seasonal prediction system for fire weather is shown in Fig. 5. This is currently based on ACCESS-S1, noting that a similar arrangement is also intended for the ACCESS-S2 model when that becomes available for BoM operational seasonal prediction purposes. It can be used to calculate fire weather indices such as the FFDI as presented here, also noting that this system has been designed to be adaptable for application to other indices in the future, including GFDI (which as discussed by Yeo *et al.* (2015) has similar inputs to the FFDI but rather than DF it includes fuel load estimates that can often be set to 4.5 t ha^{-1}, as well as degree of curing than can set to user-defined values). This model suite design is also being used as the foundation for the long-range fire weather products intended to be produced in coming years from the Australian Fire Danger Rating System (AFDRS) currently in development, noting some similar needs for AFDRS as for FFDI, KBDI and GFDI (such as initialisation based on recent observations relating to fuel moisture conditions, calibrated input variables, design of the real-time forecast products based on user feedback/co-design, etc.). Some of the key aspects of this suite design for producing fire weather outlook products are as follows:

- It is initialised using recent observations-based data relating to fuel moisture conditions as well as for rainfall.
- The input variables for the fire weather indices are each calibrated individually using quantile matching for

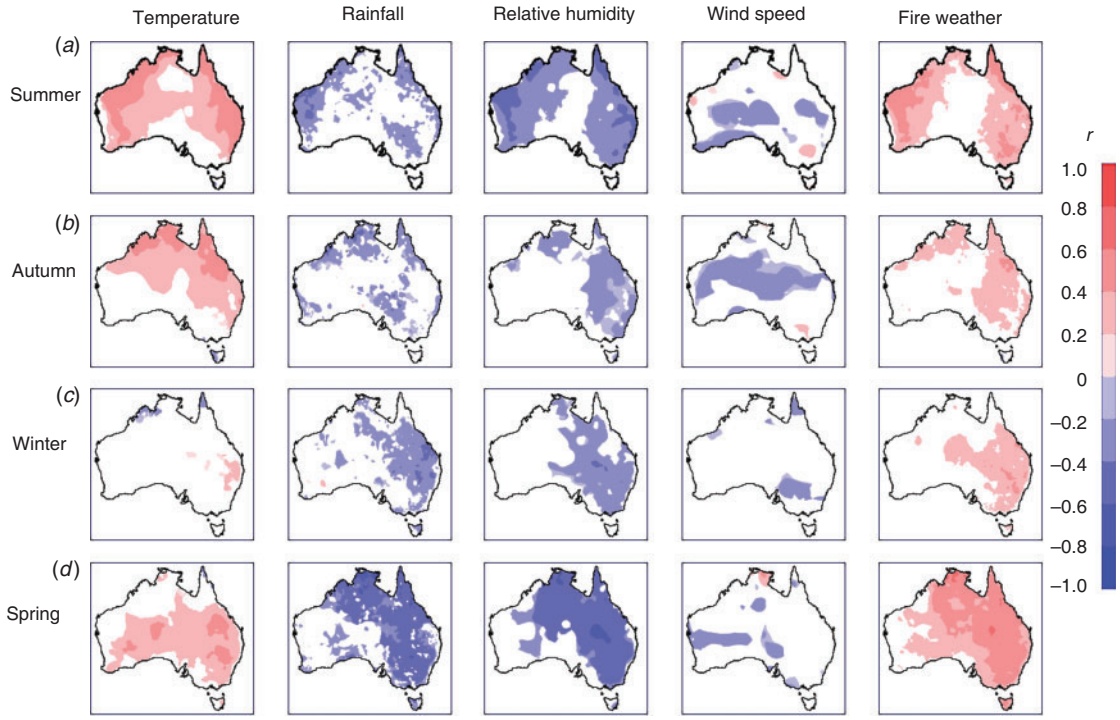

Fig. 4. Correlations between seasonal values of NINO3.4 and weather condition, including the FFDI for fire weather, for the time period from 1951 to 2016 (based on Pearson's correlation coefficient, *r*). The correlations are calculated individually for DJF (*a*), MAM (*b*), JJA (*c*) and SON (*d*). The coloured regions represent locations where the magnitude of the correlation is significant at the 95% confidence level (two-tailed).

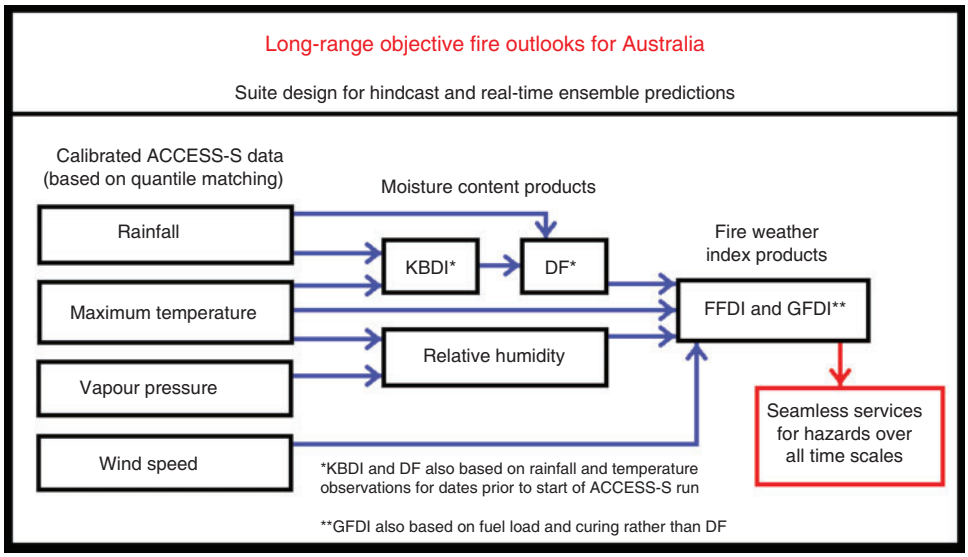

Fig. 5. Design of the suite for producing objective long-range fire weather outlooks. An overview of the key components is presented here based on the details provided in Section 3.2.

consistency with historical data sets (noting that the training period for quantile matching is that of the hindcast data from 1990 to 2012 for ACCESS-S1). Fire weather indices are then calculated based on the calibrated data (noting that subsequent calibration of the resultant index values does not appear to be important, but this would be feasible to do if need be).

For further details on data and methods including quantile matching see Section 2.

- Fire weather conditions are calculated sequentially for each day over the forecast period, using individual ensemble members (rather than using ensemble average values) for internal consistency of different weather variables which provides a better representation of dangerous combinations of variables. A range of products can be produced from this ensemble-based system, including probabilistic predictions in relation to different measures (such as the historical mean, median, terciles, etc.), depending on what the user groups may find most suitable for their applications.
- Real-time forecast products are produced for fire weather measures as well as for some variables that have previously not been available (including various measures of drought, humidity and wind speed).

The calculation of the KBDI and DF for a given day (as needed for input to the FFDI calculation in Eqn 1) is based on the previous day's values of the KBDI and the current day's temperature as well as consideration of the previous 20 days of rainfall. The design of the approach for calculating FFDI from ACCESS-S1 is based on initialising the KBDI using the most recent value of KBDI from the observations-based FFDI data set (Dowdy 2018), noting that the observations-based data set is updated automatically each day. The observations-based rainfall data are also used for input to the ACCESS-S1 calculation of KBDI and DF, but the number of days that use observed rainfall drops off with each successive day of the ACCESS-S1 forecast. For example, after 20 or more days into the forecast period from the initialisation date of ACCESS-S1 model run, no more observations-based rainfall data are used for calculating the KBDI and DF on a given day, with the previous 20 days of rainfall data being entirely based on the model output.

Building on previous results for calculating FFDI using calibrated hindcast data from ACCESS-S1 (Dowdy 2019; Dowdy *et al.* 2019), this study presents long-range FFDI predictions based on the real-time data from ACCESS-S1. Long-range predictions of FFDI are shown in Fig. 6 based on the ACCESS-S1 model output. The data were calculated for the real-time model run (50-member ensemble) initialised on 1 November 2019, with predictions shown here for each month out to February 2020. It is intended that this process will be automated in future work, so that these calculations over all ensemble members will not be needed to be produced manually each time a long-range forecast is needed. For example, guidance products based on this system are intended to be automatically updated each week or month, which could be used to provide information routinely to fire agencies. To date, these long-range fire weather prediction products have been produced quarterly for presentation to fire agencies.

These results for mean monthly FFDI show that the ACCESS-S1 values resemble the observations-based values for each of the four months of the outlook period, with the model data (Fig. 6, left panels) able to reproduce the general spatio-temporal features of mean FFDI, while noting some differences as detailed in the right-hand panels. The differences show higher FFDI values than normal values of FFDI predicted for November and December 2019, as well as into January 2020 for large areas of eastern Australia, with conditions in February being closer to normal (or lower than normal for some western and northern regions). This early summer period was characterised by very damaging fire events associated with dangerous fire weather conditions, including as indicated by observations-based FFDI values being notably higher than normal, as detailed in a Special Climate Statement published by BoM on those conditions (Bureau of Meteorology 2020).

Complementary to the mean FFDI values, probabilistic predictions were also produced, based on the probability of exceeding the mean value in a given month. This was based on the fraction of the ensemble members that produced mean FFDI values exceeding the mean values from the historical observations-based FFDI data set for that month. It is noted that in some cases this may provide complementary information to just examining the mean, including around the likelihood of the predicted outcome as compared to the magnitude. This is shown in Fig. 7, presented individually for each of the input ingredients used for calculating the FFDI, as well as for the FFDI. The predictions of a higher than normal probability of dangerous fire weather conditions (i.e. high values of FFDI) for early summer are related to the combined influence of low values of relative humidity and rainfall, as well as higher than normal temperatures, while wind speed was predicted to be slightly weaker than normal in general for Australia.

These figures were presented to all State and Territory fire agencies around Australia in mid-November 2019 as part of experimental research guidance (i.e. not an official operational BoM product), during research project meetings for a project funded by the Victorian Government Department of Environment, Land, Water and Planning (DELWP), Country Fire Authority (CFA) and BNHCRC. This project is still currently underway, with these results intended as interim results along the way to finalising the methods by the end of the project in June 2021. Given that the FFDI combines humidity and wind speed together with temperature and rainfall information into a single integrated measure that includes antecedent information for fuel moisture, it provided complementary guidance to the official operational seasonal outlooks of temperature and of rainfall that were also provided to fire agencies, for helping their planning leading into the 2019–2020 summer. The fire weather conditions that ended up occurring were a lot more severe than normal for this period leading into the summer, including FFDI value considerably higher than normal throughout large areas of Australia during December and into early January (BoM 2020).

The ACCESS-S1 hindcast consists of an 11-member ensemble in each year from 1990 to 2012 and can be useful for model validation as detailed in Hudson *et al.* (2017). The long-range predictions of FFDI shown in Fig. 6 for the 2019–2020 summer use the model run from 1 November 2019. To examine the skill of the model in making predictions such as this for the summer fire season in southern Australia, Fig. 8 shows hindcast predictions for model runs from 1 November in each of the years from 1990 to 2012. The predictions shown are for ensemble average FFDI values through southern Australia (average for all land locations south of 27°S). Predictions of above or below median are correct for about three quarters of those years (74%),

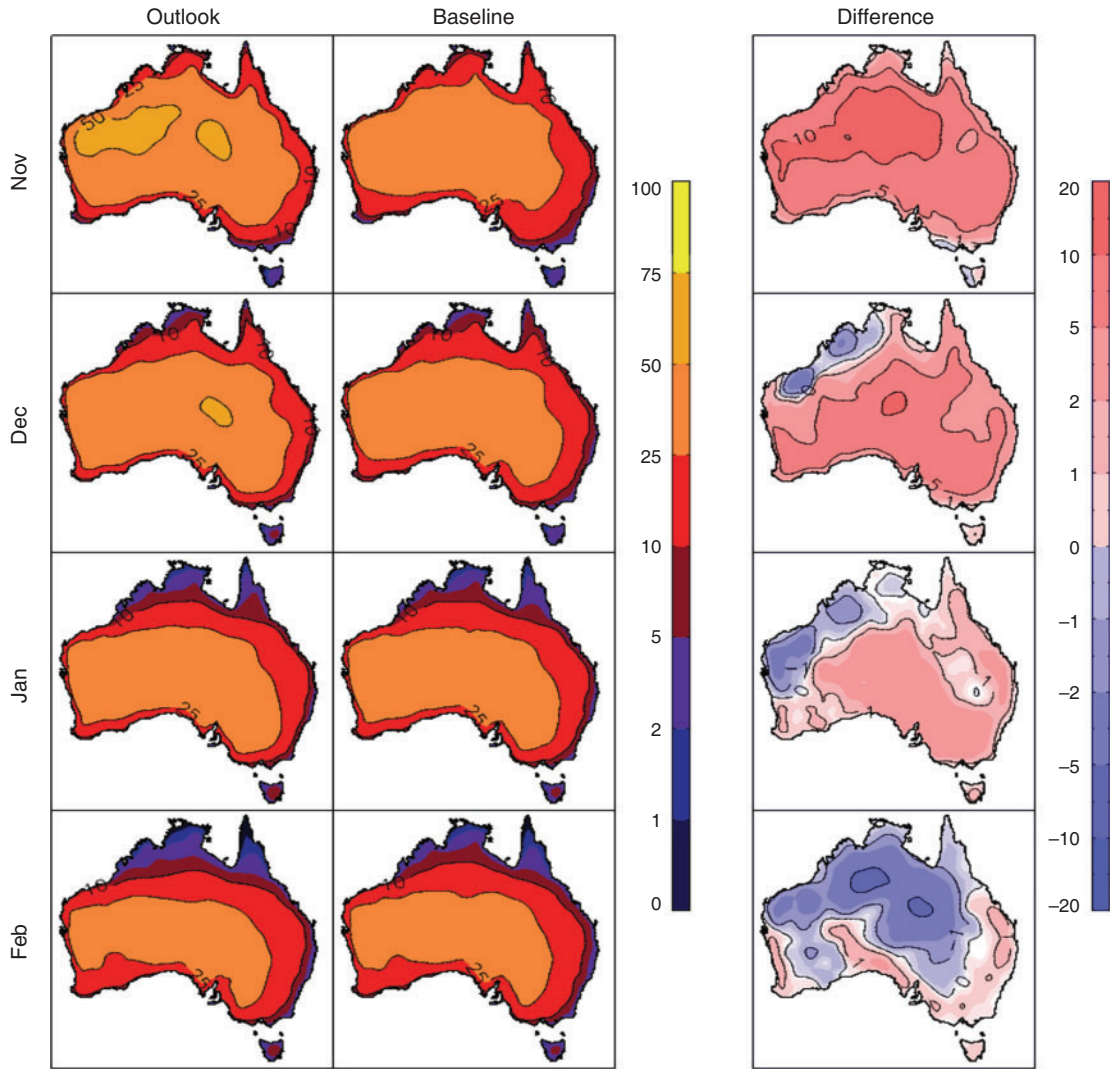

Fig. 6. Long-range prediction of FFDI values based on ACCESS-S1 model initialised on 1 November 2019. Results are shown for individual months (from November 2019 to February 2020 in each row, respectively) for the mean FFDI based on the model (left panels) and based on observations over the past 30 years from 1989–2018 (middle panel), with their difference also presented (right panels).

assessed in relation to the observations-based FFDI data described in Dowdy (2018).

3.3 The 2019–2020 summer fires and use of seamless products

A large number of extremely dangerous fires occurred during the 2019–2020 summer, burning huge areas of eastern and southern Australia, as well as tragically resulting in many deaths and the destruction of built and natural environments. This suite of seamless fire weather products was used extensively in relation to this fire season prior to, during and after the summer. Some examples of this are provided here, highlighting a range of tangible benefits resulting from these calibrated data sets, including around improved preparedness, communication and understanding of the extremely dangerous fire weather conditions that occurred.

As detailed in Section 3.2, long-range fire weather guidance based on real-time ACCESS-S1 ensemble predictions was provided to state fire management authorities in mid-November 2019 (including Figs 6 and 7), clearly indicating the higher than normal chance of dangerous weather conditions in the coming months into January 2020. This research product was the first time that these long-range fire weather predictions were available prior to the summer period for Australia, as previously the information based on ACCESS-S model output was focused on temperature and rainfall individually (rather than combined together with humidity and wind speed into an integrated fire weather measure). This helped provide additional lines of evidence for climate research-based guidance on upcoming conditions, in addition to the official operational products based on temperature and rainfall for their planning around the upcoming period (from multiple weeks to months

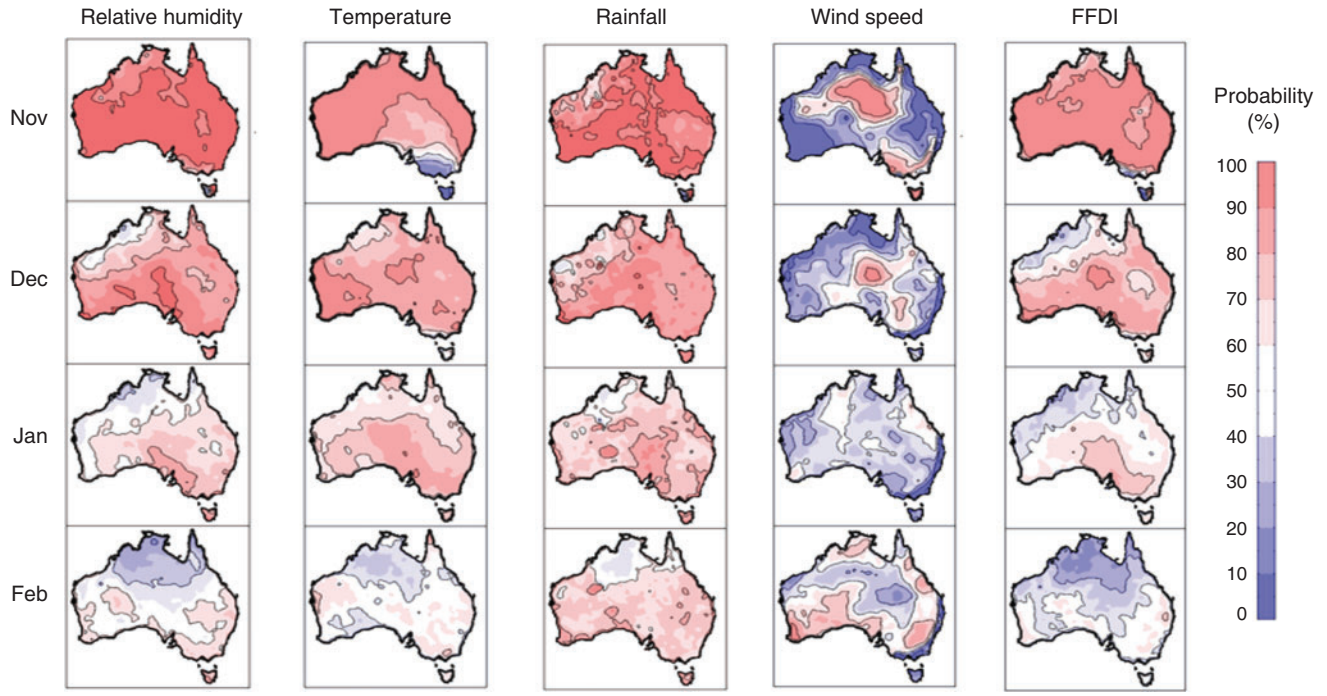

Fig. 7. Long-range prediction of weather variables used for calculating the FFDI, as well as the FFDI. Results are presented as the probability of exceeding the mean value, based on the fraction of the model ensemble members that have means values higher than that of the historical observations-based FFDI data set. Red colours correspond to conditions associated with higher FFDI values and blue colours correspond to conditions associated with lower FFDI values, corresponding to higher temperature and wind speed values as well as lower relative humidity and rainfall values (shown in each respective column). This is based on ACCESS-S1 model initialised on 1 November 2019. Results are shown for individual months from November 2019 to February 2020 in each row, respectively.

ahead, noting that some decisions can benefit from long-range guidance such as ordering of aircraft and arranging for additional fire fighters from other regions).

Information on the observed climate change trends as well as future climate projections based on these calibrated data was provided to state agencies, the BNHCRC and the Australasian Fire and Emergency Service Authorities Council (AFAC) and their partner agencies in the spring of 2019. This information highlighted an increased likelihood in recent years of conditions that are more severe than ever experienced previously, particularly during spring and summer in parts of southern and eastern Australia. Consequently, this suggests that changes in planning and preparedness may be beneficial to consider, including leading into the fire season in these regions, to help enable enhanced resilience to conditions potentially more severe than those in the historical records and the previous experience of fire fighters and fire management groups.

During the summer period, the historical data set of FFDI (updated automatically each day) was used numerous times for guidance on understanding the severity of conditions associated with the fire events that occurred. This included being able to provide insight on the severity of the conditions based on a long historical context (back to 1950, including enabling comparisons with daily maps of FFDI for other notable historical events such as Black Saturday, Ash Wednesday and others) as well as being able to indicate regional features given that it is based on a gridded analysis of observations data (e.g. complementary to station-based data). Many examples of conditions were found to be unprecedented in the 70-year historical record, such as detailed in the Special Climate Statements produced by BoM during the summer as events unfolded, including record high individual daily values as well as record high monthly average values of FFDI in many parts of the country (Bureau of Meteorology 2019*a*, 2019*b*, 2020). Being able to document and analyse conditions in this way helped enhance communication around the severity and anomalous nature of the conditions that were occurring.

The suite of calibrated fire weather data sets was also used extensively in post-summer analysis and inquiries, including for four individual state inquiries as well as for the Royal Commission into National Natural Disaster Arrangements (Australian Government 2020). For example, the BoM presentation on the first day of the Royal Commission (https://naturaldisaster.royalcommission.gov.au/system/files/exhibit/BOM.502.001.0001_0.pdf) showed many figures based on the historical FFDI data set, as well as some based on the future projections data set calibrated to match the historical data set. Slide 76 of that presentation (also included as Fig. A2 in the Appendix) shows maps of FFDI using the observations-based data for three days from January 2020 on which extremely dangerous fire events occurred, as well as using the calibrated projections data from one individual model to show three days from January 2050 for the future simulated climate

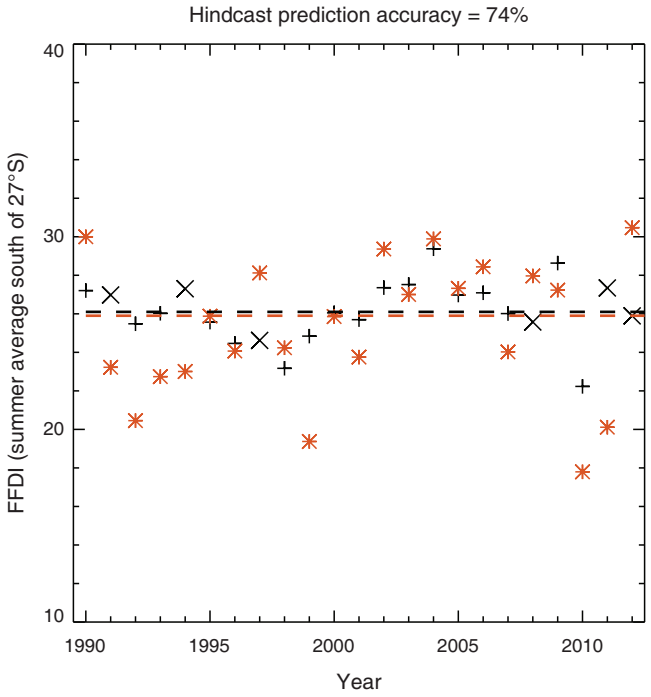

Fig. 8. ACCESS-S1 hindcast values of FFDI based on the 1 November model runs, to examine predictions for the southern fire season during summer. Average values of FFDI are shown for December, January and February in land regions south of 27°S latitude through Australia, including for the hindcast predictions (black symbols), as well as for the gridded observations-based FFDI data (orange symbols) as described by Dowdy (2018). Ensemble average predictions are shown for each year, with those predictions assessed in relation to being above or below the median values (horizontal dashed lines). The accuracy of those predictions is 74% based on the fraction of correct predictions ('+' symbols for correct predictions) from these 23 years, using the observations-based values as the reference data set for that assessment.

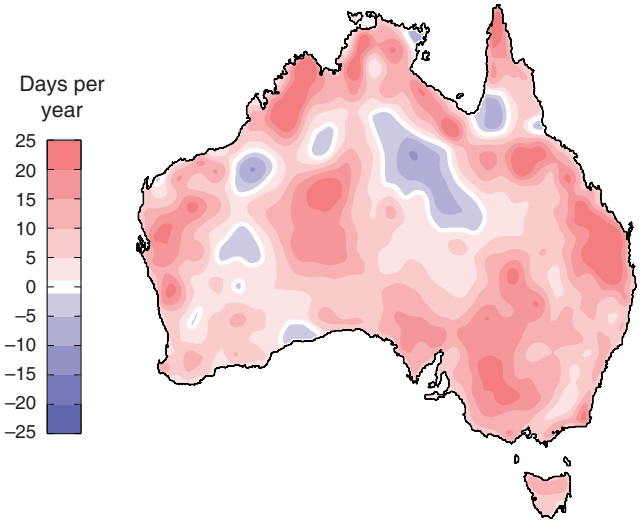

Fig. 9. Long-term change in the average number of days per year that have FFDI > 90th percentile. This is shown for the change from the period July 1950–June 1985 to the period July 1985–June 2020, using the methods and data set as described in Dowdy (2018).

(as an example of one future simulated extreme event for comparison with the extreme conditions experience during the 2019–2020 summer). As the first presentation of the Royal Commission, the gridded fire weather data sets over different time scales helped set the scene and provide the scientific context around the extremely dangerous conditions and destructive fire events that occurred, noting that the outcomes of the Royal Commission are intended to enhance future planning and preparedness efforts to reduce the impacts of future extreme fire events on Australian society and environment.

There are various other examples of how this broader set of consistent fire weather products was used in the inquiries following the 2019–2020 summer. Examples for future projected changes include Fig. 6 of the Royal Commission final report (Australian Government 2020). The GCM data in that figure have the QME method applied for consistency with the gridded observations-based FFDI data set (Dowdy 2018) and are the same projections data used here in Fig. 2 showing projections for FFDI > 50 (whereas the version in the Royal Commission report provides projections for FFDI > 25 as presented in Dowdy *et al.* (2019)). That gridded observations-based FFDI data set was also presented in various inquiries, such as for examining historical changes in figures 2–23 and 2–24 of the NSW inquiry report (NSW Government 2020) and Fig. 7 of the inquiry report for South Australia (Government of South Australia 2020), with an updated map of historical changes shown in Fig. 9 using that data set.

4 Summary

Fire weather data sets are now available in a consistent form covering historical records back to 1950, long-range predictions out to several months ahead and future climate projections through to the end of this century. All of these datasets use a 0.05° grid spacing in both latitude and longitude, with daily values of various fire weather indices (e.g. FFDI, DF, KBDI as well as individual input ingredients for weather conditions), with the model-based data calibrated to match the historical observations-based gridded data sets using quantile matching.

The results presented here highlight the benefits of seamless fire weather guidance products for fire management applications in Australia. This includes based on calibrated output from GCMs for future climate change projections (Section 3.1) and the ACCESS-S1 model currently used by the BoM for long-range prediction activities (Section 3.2). Calibration based on quantile matching with care around extremes was applied here to help with the provision of seamless predictions across scales that are also consistent with the historical records. The production of FFDI values based on ACCESS-S1 real-time values is currently in the process of being automated to run each day using this system design as described above (Section 3.2), noting a similar automation of the historical FFDI data set which is currently producing daily updates. Future work is planned to shift this long-range prediction suite to ACCESS-S2 (the planned successor to ACCESS-S1) when data become available,

as well as building on this suite design for other fire weather measures such as those planned for the upcoming Australia Fire Danger Rating System (AFDRS). Climate projections of FFDI do not need updating as frequently as the seasonal prediction and historical data sets, but it is intended that an update will occur when the CMIP6 data become more readily available in the future as well as based on available regional downscaling from GCM data (e.g. Di Virgilio *et al.* 2019; Dowdy *et al.* 2019).

Projections of FFDI in future simulated climates under different greenhouse gas emission pathways provide one indication of how dangerous fire conditions could change in the future, while noting that future fire occurrence can be influenced by many different factors including a broad range of weather-related as well as other factors (such as land-use changes, climate adaptation activities, etc.). The FFDI is useful for providing a general indication of near-surface weather conditions and fuel moisture that can influence fire behaviour (broadly similar to a range of other indices used around the world for fire management applications). Complementary to near-surface indices, the C-Haines index provides an indication of conditions at higher levels of the atmosphere that can also be associated with dangerous fire events such as those that can generate thunderstorms in their fire plumes (i.e. pyrocumulonimbus clouds, pyroCb) with recent studies showing a potential increase in such risk factors in parts of southern and southeastern Australia (Dowdy and Pepler 2018; Di Virgilio *et al.* 2019; Dowdy *et al.* 2019). Another weather-related factor is ignition risk from dry-lightning (i.e. lightning that occurs with little rainfall, less than about 2.5 mm), with analysis over recent decades indicating decreases in dry-lightning frequency for many parts of Australia as well as increases in parts of southeast Australia (Dowdy 2020). Consequently, in addition to the extreme measures presented in Fig. 2 of this study, there are various other lines of evidence that highlight southern Australia as having a concentration of increased risk factors for bushfires in a warming world.

This suite of calibrated fire weather products described here is being used extensively, including some examples provided here, in relation to the extreme fire conditions during the 2019–2020 summer. Calibrated model data provide scope for a wide range of improved guidance products based on these weather factors. The ACCESS-S FFDI values enable relative humidity, wind speed and soil moisture (KBDI) predictions at long range, given that these are input ingredients of the FFDI, noting relatively limited products to date in relation to such variables. Similarly, for the future climate projections, the various input ingredients to the FFDI provide scope for improved understanding of projected future changes in various aspects of weather and climate based on calibrated data consistent with observations-based data sets.

Conflicts of interest

The author declares no conflicts of interest.

Acknowledgements

This work was supported by the ESCC Hub of the Australian Government's National Environmental Science Program (NESP) as well as the ERP14 project funded through DELWP/CFA/BNHCRC. Comments on earlier drafts by Hanh Nguyen and Surendra Rauniyar from Bureau of Meteorology are gratefully acknowledged.

References

Australian Government (2020). Royal Commission into National Natural Disaster Arrangements. Australian Government, Canberra

Bedia, J., Golding, N., Casanueva, A., Iturbide, M., Buontempo, C., and Gutiérrez, J. M. (2018). Seasonal predictions of Fire Weather Index: Paving the way for their operational applicability in Mediterranean Europe. *Climate Serv.* **9**, 101–110. doi:10.1016/J.CLISER.2017.04.001

Blanchi, R., Lucas, C., Leonard, J., and Finkele, K. (2010). Meteorological conditions and wildfire-related houseloss in Australia. *Int. J. Wildland Fire* **19**(7), 914–926. doi:10.1071/WF08175

Blanchi, R., Leonard, J., Haynes, K., Opie, K., James, M., and Oliveira, F. D. (2014). Environmental circumstances surrounding bushfire fatalities in Australia 1901–2011. *Environ. Sci. Policy* **37**, 192–203. doi:10.1016/J.ENVSCI.2013.09.013

Boer, M. M., Resco de dios, V., and Bradstock, R. A. (2020). Unprecedented burn area of Australian mega forest fires. *Nature Climate Change* **10**(3), 171–172. doi:10.1038/S41558-020-0716-1

Bradstock, R. A., Cohn, J. S., Gill, A. M., Bedward, M., and Lucas, C. (2009). Prediction of the probability of large fires in the Sydney region of south-eastern Australia using fire weather. *Int. J. Wildland Fire* **18**(8), 932–943. doi:10.1071/WF08133

Bureau of Meteorology (2019). Forecasting for the Future: New science for improved weather, water, ocean and climate services – Abstracts of the Bureau of Meteorology Annual R&D Workshop, 25–28 November 2019, Melbourne, Australia. Bureau of Meteorology, Victoria, Australia. Research Report No. 40. Available at http://www.bom.gov.au/research/publications/researchreports/BRR-040.pdf

Bureau of Meteorology (2019*a*). Special Climate Statement 71. Bureau of Meteorology, Victoria, Australia. Available at http://www.bom.gov.au/climate/current/statements/scs71.pdf

Bureau of Meteorology (2019*b*). Special Climate Statement 72. Bureau of Meteorology, Victoria, Australia. Available at http://www.bom.gov.au/climate/current/statements/scs72.pdf

Bureau of Meteorology (2020). Special Climate Statement 73. Bureau of Meteorology, Victoria, Australia. Available at http://www.bom.gov.au/climate/current/statements/scs73.pdf

Casanueva, A., Herrera, S., Iturbide, M., Lange, S., Jury, M., Dosio, A., Maraun, D., and Gutiérrez, J. M. (2020). Testing bias adjustment methods for regional climate change applications under observational uncertainty and resolution mismatch. *Atmos Sci Lett.* **21**, e978. doi:10.1002/ASL2.V21.7

Chen, Y., Morton, D. C., Andela, N., Giglio, L., and Randerson, J. T. (2016). How much global burned area can be forecast on seasonal time scales using sea surface temperatures?. *Environ. Res. Lett.* **11**(4), 045001. doi:10.1088/1748-9326/11/4/045001

Chikamoto, Y., Timmermann, A., Widlansky, M. J., Balmaseda, M. A., and Stott, L. (2017). Multi-year predictability of climate, drought, and wildfire in southwestern North America. *Sci. Rep.* **7**(1), 6568. doi:10.1038/S41598-017-06869-7

Clarke, H., Pitman, A. J., Kala, J., Carouge, C., Haverd, V., and Evans, J. P. (2016). An investigation of future fuel load and fire weather in Australia. *Clim. Change* **139**(3), 591–605. doi:10.1007/S10584-016-1808-9

CSIRO and BoM (2015). Climate Change in Australia Information for Australia's Natural Resource Management Regions: Technical Report. CSIRO and Bureau of Meteorology, Australia. Available at

https://www.climatechangeinaustralia.gov.au/media/ccia/2.1.6/cms_page_media/168/CCIA_2015_NRM_TechnicalReport_WEB.pdf

Di Virgilio, G., Evans, J. P., Blake, S. A. P., Armstrong, M., Dowdy, A. J., Sharples, J., and McRae, R. (2019). Climate change increases the potential for extreme wildfires. *Geophys. Res. Lett.* **46**(14), 8517–8526. doi:10.1029/2019GL083699

Dowdy, A. J. (2018). Climatological variability of fire weather in Australia. *J. Appl. Meteorol. Climatol.* **57**, 221–234. doi:10.1175/JAMC-D-17-0167.1

Dowdy, A. J. (2019). Towards seamless predictions across scales for fire weather. Proceedings for the 6th International Fire Behaviour and Fuels Conference, 2019, Sydney, Australia. Published by the International Association of Wildland Fire, Missoula, Montana, USA. Available at http://albuquerque.firebehaviorandfuelsconference.com/wp-content/uploads/sites/13/2019/04/Dowdy-Sydney.pdf

Dowdy, A. J. (2020). Climatology of thunderstorms, convective rainfall and dry lightning environments in Australia. *Climate Dyn.* **54**(5), 3041–3052. doi:10.1007/S00382-020-05167-9

Dowdy, A. J., and Pepler, A. (2018). Pyroconvection risk in Australia: Climatological changes in atmospheric stability and surface fire weather conditions. *Geophys. Res. Lett.* **45**(4), 2005–2013. doi:10.1002/2017GL076654

Dowdy, A. J., Field, R. D., and Spessa, A. C. (2016). Seasonal forecasting of fire weather based on a new global fire weather database. Proceedings for the 5th International Fire Behaviour and Fuels Conference, 11–15 April 2016, Melbourne, Australia. International Association of Wildland Fire, Missoula, Montana, USA

Dowdy, A., Ye, H., Tory, K., Jones, D., Evans, A., Lavender, S., Thatcher, M., Rafter, T., Osbrough, S., Walsh, K., Cavicchia, L., Evans, J., and Catto, J. (2017). Extreme weather: improved data products on bushfires, thunderstorms, tropical cyclones and east coast lows. In 'Bushfire and Natural Hazards CRC & AFAC Conference' (Ed. I. M. Rumsewicz.) Bushfire and Natural Hazards CRC, Sydney. Available at http://nespclimate.com.au/wp-content/uploads/2016/03/AFAC2017-climate_extremes.pdf

Dowdy, A. J., Ye, H., Pepler, A., Thatcher, M., Osbrough, S. L., Evans, J. P., Di Virgilio, G., and McCarthy, N. (2019). Future changes in extreme weather and pyroconvection risk factors for Australian wildfires. *Sci. Rep.* **9**(1), 10073. doi:10.1038/S41598-019-46362-X

Garfin, G. M., Brown, T. J., Wordell, T., and Delgado, E. (2016). The making of national seasonal wildfire outlooks. In 'Climate in Context: Science and Society Partnering for Adaptation' (Eds A. S. Parris, G. M. Garfin, K. Dow, R. Meyer, S. L. Close) pp.143–172. (Wiley)

Government of South Australia (2020). Independent Review into South Australia's 2019–20 bushfire season. Government of South Australia. Available at https://www.safecom.sa.gov.au/site/independent_review_sa_201920_bushfires.jsp

Harris, S., and Lucas, C. (2019). Understanding the variability of Australian fire weather between 1973 and 2017. *PloS One* **14**(9), e0222328. doi:10.1371/JOURNAL.PONE.0222328

Harris, S., Nicholls, N., Tapper, N., and Mills, G. (2019). The sensitivity of fire activity to interannual climate variability in Victoria, Australia. *J. South. Hemisph. Earth Syst. Sci.* **69**(1), 146–160. doi:10.1071/ES19008

Hertig, E., Maraun, D., Bartholy, J., Pongracz, R., Vrac, M., Mares, I., Gutiérrez, J. M., Wibig, J., Casanueva, A., and Soares, P. M. M. (2019). Comparison of statistical downscaling methods with respect to extreme events over Europe: Validation results from the perfect predictor experiment of the COST Action VALUE. *Int. J. Climatol.* **39**(9), 3846–3867. doi:10.1002/JOC.5469

Hudson, D., Alves, O., Hendon, H. H., *et al.* (2017). ACCESS-S1 the new Bureau of Meteorology multi-week to seasonal prediction system. *J. South. Hemisph. Earth Syst. Sci.* **67**(3), 132–159. doi:10.22499/3.6703.001

IPCC (2013). Summary for Policymakers. In 'Climate Change 2013: The Physical Science Basis. Contribution of Working Group I to the Fifth Assessment Report of the Intergovernmental Panel on Climate Change' (Eds T. F. Stocker, D. Qin, G.-K. Plattner, M. Tignor, S. K. Allen, J. Boschung, A. Nauels, Y. Xia, V. Bex and P. M. Midgley). Cambridge University Press, Cambridge, United Kingdom and New York, NY, USA.

IPCC (2018). Global Warming of 1.5°C. An IPCC Special Report on the impacts of global warming of 1.5°C above pre-industrial levels and related global greenhouse gas emission pathways, in the context of strengthening the global response to the threat of climate change, sustainable development, and efforts to eradicate poverty (Eds V. Masson-Delmotte, and Coauthors)

Johnston, F. H., Borchers-Arriagada, N., Morgan, G. G., Jalaludin, B., Palmer, A. J., Williamson, G. J., and Bowman, D. M. J. S. (2020). Unprecedented health costs of smoke-related PM 2.5 from the 2019–20 Australian megafires. *Nat. Sustain.* doi:10.1038/S41893-020-00610-5

Jones, D., Wang, W., and Fawcett, R. (2009). High-quality spatial climate datasets for Australia. *Aust. Meteorol. Mag.* **58**, 233–248.

Keetch, J. J., and Byram, G. M. (1968). A drought index for forest fire control. Res. Pap. SE-38. Asheville, NC: U.S. Department of Agriculture, Forest Service, Southeastern Forest Experiment Station

King, A. D., Alexander, L. V., and Donat, M. G. (2013). The efficacy of using gridded data to examine extreme rainfall characteristics: a case study for Australia. *Int. J. Climatol.* **33**(10), 2376–2387. doi:10.1002/joc.3588

Lim, E. P., Hendon, H. H., Boschat, G., Hudson, D., Thompson, D. W. J., Dowdy, A. J., and Arblaster, J. M. (2019). Australian hot and dry extremes induced by weakenings of the stratospheric polar vortex. *Nat. Geosci.* **12**(11), 896–901. doi:10.1038/S41561-019-0456-X

Luke, R. H., and McArthur, A. G. (1978). Bushfires in Australia. Australian Government Publishing Service, ISBN 0642039909

McArthur, A. G. (1967). Fire behaviour in eucalypt forests. Forestry and Timber Bureau, Canberra

Meinig, D. W. (1961). Goyder's line of rainfall: The role of a geographic concept in South Australian land policy and agricultural settlement. *Agricultural History* **35**(4), 207–214.

Moise, A., Wilson, L., Grose, M., Whetton, P., Watterson, I., Bhend, J., Bathols, J., Hanson, L., Erwin, T., Bedin, T., and Heady, C. (2015). Evaluation of CMIP3 and CMIP5 models over the Australian region to inform confidence in projections. *Aust. Meteorol. Oceanogr. J.* **65**(1), 19–53. doi:10.22499/2.6501.004

Nicholls, N., and Lucas, C. (2007). Interannual variations of area burnt in Tasmanian bushfires: relationships with climate and predictability. *Int. J. Wildland Fire* **16**(5), 540–546. doi:10.1071/WF06125

Nidumolu, U., Hayman, P., Howden, S., and Alexander, B. (2012). Re-evaluating the margin of the South Australian grain belt in a changing climate. *Climate Res.* **51**(3), 249–260. doi:10.3354/CR01075

Noble, I. R., Gill, A. M., and Bary, G. A. V. (1980). McArthur's fire-danger meters expressed as equations. *Aust. J. Ecol.* **5**(2), 201–203. doi:10.1111/J.1442-9993.1980.TB01243.X

NSW Government (2020). Final Report of the NSW Bushfire Inquiry. NSW Government. Available at https://www.dpc.nsw.gov.au/publications/categories/nsw-bushfire-inquiry/

Taylor, K. E., Stouffer, R. J., and Meehl, G. A. (2012). An Overview of CMIP5 and the experiment design. *Bull. Amer. Meteor. Soc.* **93**, 485–498. doi:10.1175/BAMS-D-11-00094.1

Tozer, C., Verdon-Kidd, D., and Kiem, A. (2014). Temporal and spatial variability of the cropping limit in South Australia. *Climate Res.* **60**(1), 25–34. doi:10.3354/CR01218

Turco, M., Jerez, S., Doblas-Reyes, F. J., AghaKouchak, A., Llasat, M. C., and Provenzale, A. (2018). Skilful forecasting of global fire activity

using seasonal climate predictions. *Nat. Commun.* **9**(1), 2718. doi:10.1038/S41467-018-05250-0

Ward, M., Tulloch, A. I. T., Radford, J. Q., Williams, B. A., Reside, A. E., Macdonald, S. L., Mayfield, H. J., Maron, M., Possingham, H. P., Vine, S. J., and O'Connor, J. L. (2020). Impact of 2019–2020 mega-fires on Australian fauna habitat. *Nat. Ecol. Evol.* **4**(10), 1321–1326. doi:10.1038/S41559-020-1251-1

Williams, A. A. J., Karoly, D. J., and Tapper, N. (2001). The sensitivity of Australian fire danger to climate change. *Clim. Change* **49**(1), 171–191. doi:10.1023/A:1010706116176

Yeo, C. S., Kepert, J. D., and Hicks, R. (2015). Fire danger indices: current limitations and a pathway to better indices. Bushfire & Natural Hazards CRC, Melbourne, Australia, BNHCRC Report Number 2014.007

Appendix A – Supplementary information

Table A1. Details on the global climate models used here, including horizonal grid spacing and number of vertical levels (further details in Moise *et al.* 2015)

Model name	Horizontal grid spacing (degrees latitude × longitude)	Vertical resolution (number of levels)
ACCESS1-0	1.9 × 1.2	38
ACCESS1-3	1.9 × 1.2	38
BCC-CSM1-1	2.8 × 2.8	26
BCC-CSM1-1-M	1.12 × 1.12	26
BNU-ESM	2.8 × 2.8	26
CCSM4	1.25 × 0.94	26
CNRM-CM5	1.4 × 1.4	31
CSIRO-Mk3-6-0	1.8 × 1.8	18
FGOALS-G2	2.8 × 2.8	26
GFDL-CM3	2.5 × 2.0	48
GFDM-ESM2G	2.5 × 2.0	24
GFDM-ESM2M	2.5 × 2.0	24
MIROC5	1.4 × 1.4	40
MRI-CGCM3	1.1 × 1.1	48
NorESM1-M	2.5 × 1.9	26

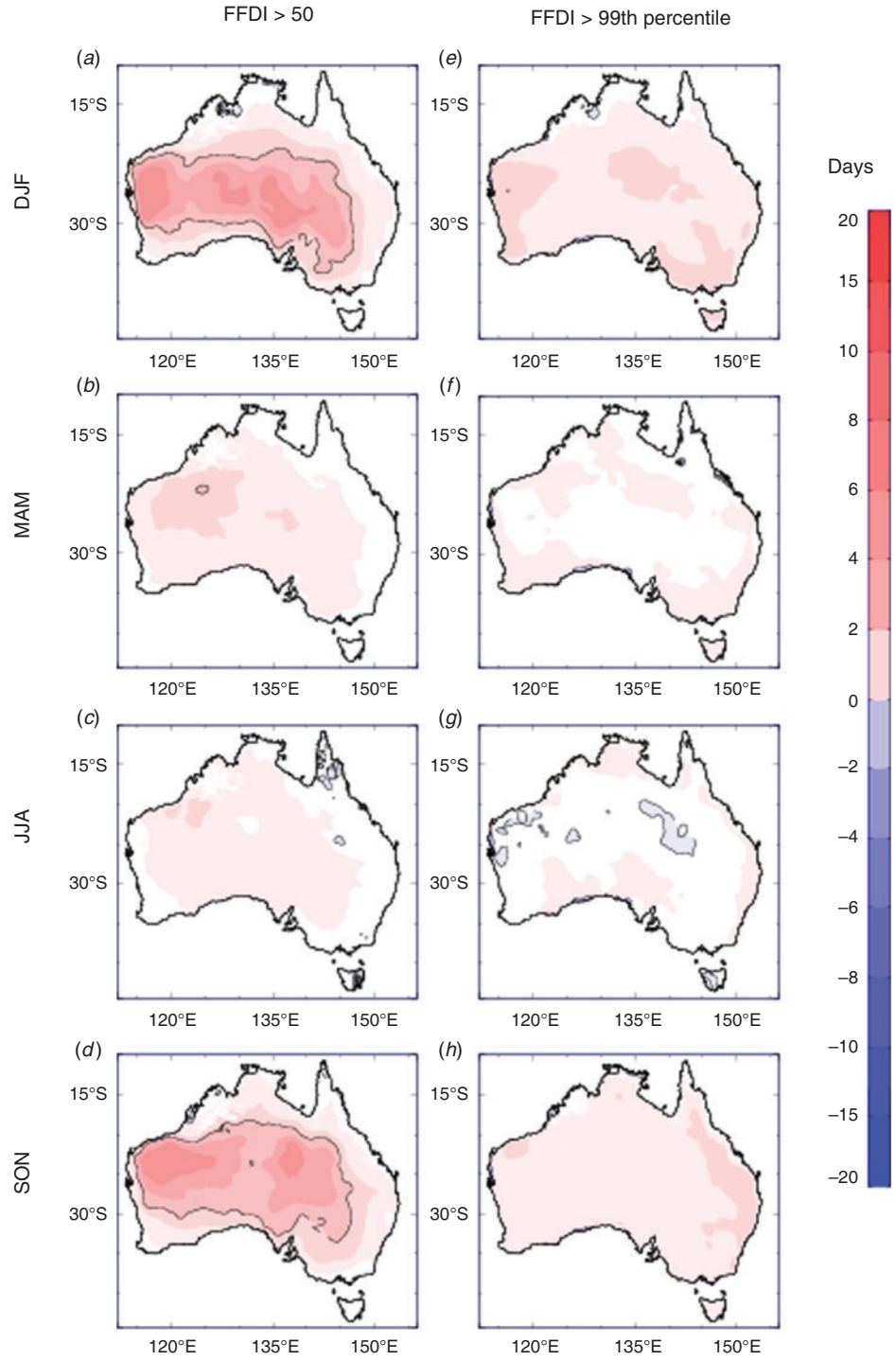

Fig. A1. As for Fig. 2, but for near-term climate projections. Future projections in FFDI values from the calibrated GCM data. Changes are shown for the number of days per year that the FFDI exceeds a threshold value, based on changes from the period 1990–2009 to the period 2020–2039. Results are presented for the number of days per year that FFDI is above 50 (left panels, *a*–*d*) and the number of days per year that FFDI is above its historical period 99th percentile (right panels, *e*–*h*). This is shown for individual seasons DJF (*a*, *e*), MAM (*b*, *f*), JJA (*c*, *g*) and SON (*d*, *h*).

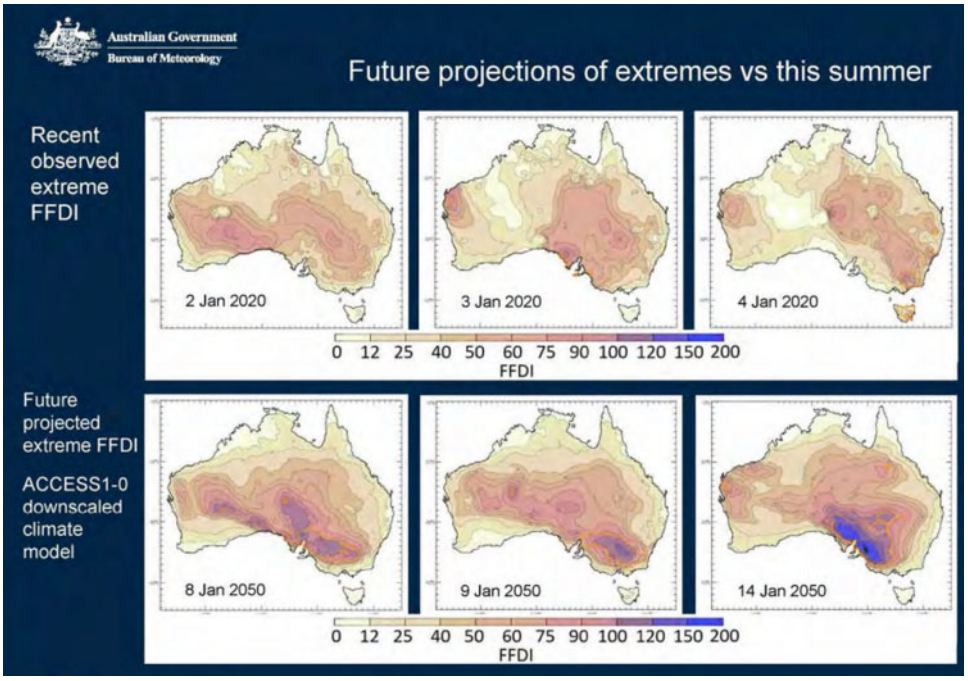

Fig. A2. Example from BoM presentation on Day 1 of the Royal Commission, as slide 67 of the full presentation available here https://naturaldisaster.royalcommission.gov.au/system/files/exhibit/BOM.502.001.0001_0.pdf. Maps of daily FFDI are shown using the observations-based data set (Dowdy 2018) for three individual days from January 2020 on which extremely dangerous fire events occurred, as well as using the QME calibrated FFDI projections data set (Dowdy *et al.* 2019) for the ACCESS1-0 GCM to show three individual days from January 2050 for the future simulated climate. These days were selected to highlight a future simulated extreme event for comparison with some of the extreme conditions experienced during the 2019–2020 summer.

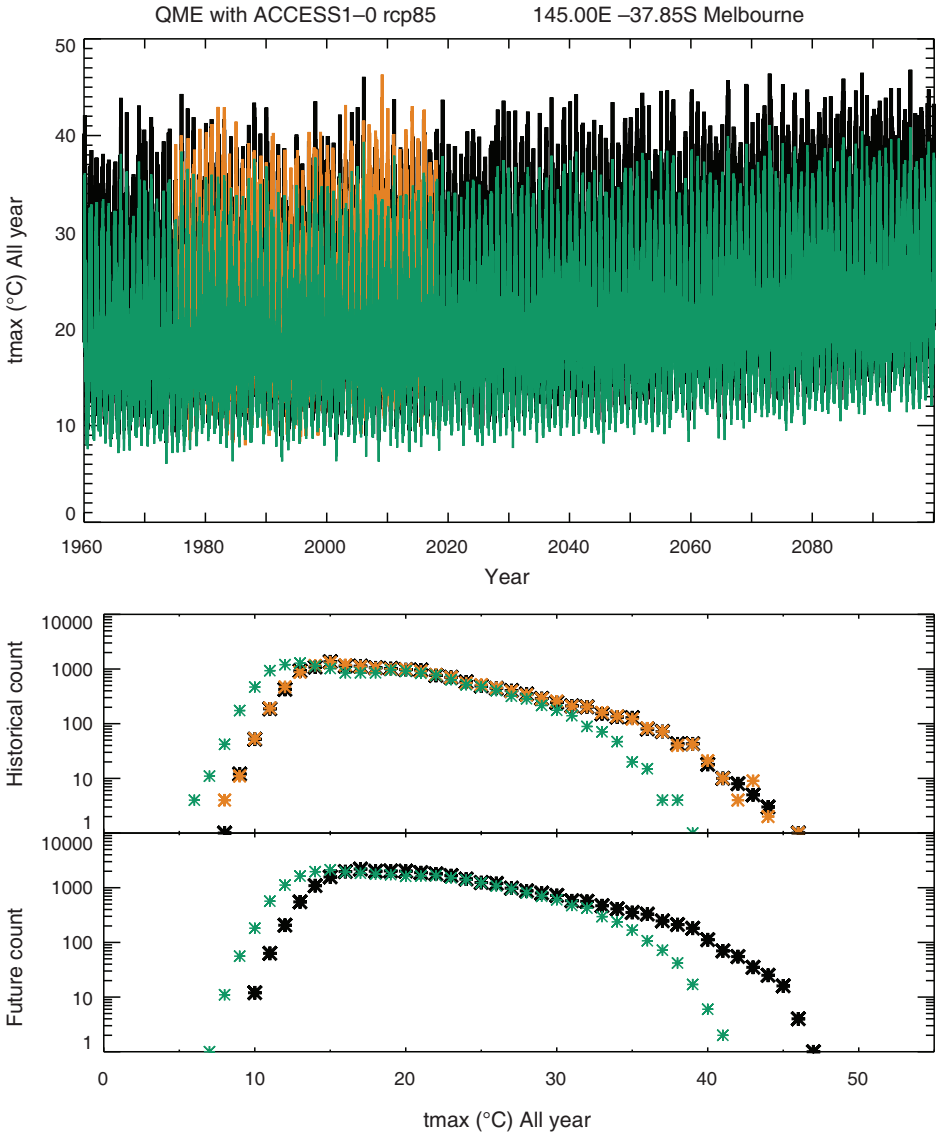

Fig. A3. Example of applying the QME calibration method to the global climate model ACCESS1-0 historical and RCP8.5 simulations. Results are presented for daily values of maximum temperature at a height of 2 m in Melbourne (using a grid cell of 0.05° in latitude and longitude corresponding to 145.00°E and 37.85°S). The direct output data from the model is shown (green) and the bias-corrected version of these data (black), together with the AWAP gridded analysis of observations data used to train the method (orange). Time series are shown (upper panel), as well as PDFs for the training period from 1975 to 2017 (middle panel) and projections for 2018 to 2100 (lower panel).

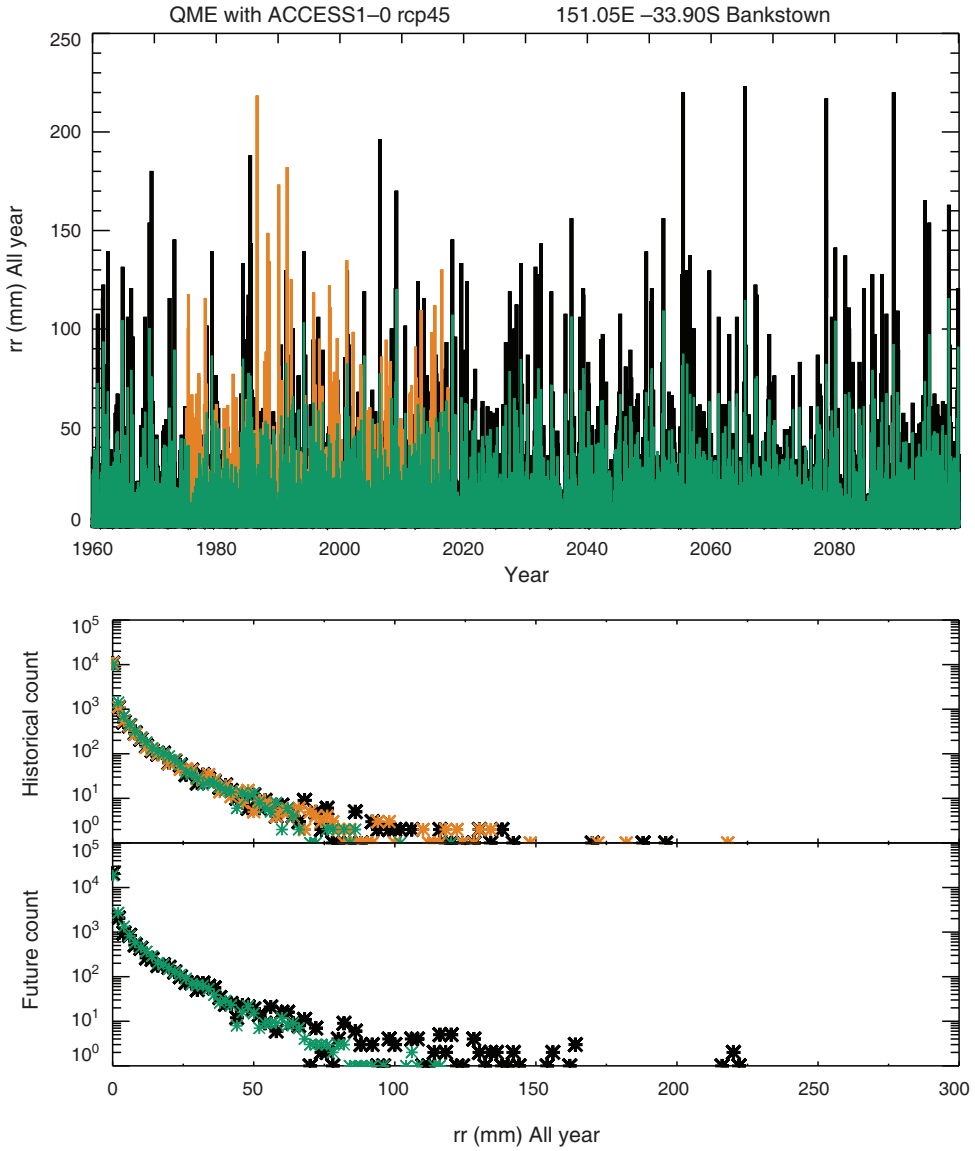

Fig. A4. As for Fig. A3 but for rainfall in Bankstown, Sydney (using a grid cell of 0.05° in latitude and longitude corresponding to 151.05°E, 33.90°S).